

# Morphological control in solvothermal synthesis of copper sulphides on copper foil

S. Gorai, D. Ganguli, S. Chaudhuri \*

*Department of Materials Science, Indian Association for the Cultivation of Science, Kolkata 700032, India*

Received 6 December 2005; received in revised form 17 May 2006; accepted 29 May 2006

Available online 7 July 2006

---

## Abstract

Copper sulphides  $\text{Cu}_9\text{S}_5$  and polymorphs of  $\text{Cu}_2\text{S}$  were synthesized apparently for the first time on copper foil through its solvothermal reaction with sulphur (the former being used both as substrate and reactant), with 75% fill of the autoclave with water, ethanol or ethylenediamine as solvents. Water as solvent produced micron-sized hemispheres of  $\text{Cu}_9\text{S}_5$  (composed of much smaller particles of size  $\sim 5\text{--}6\text{ nm}$ ), truncated by forming interfaces and exhibiting relatively large dihedral angles ( $80\text{--}120^\circ$ ). Ethanol produced fibre-like or thread-like ( $\sim 40\text{ nm}$  diameter) morphological form of  $\text{Cu}_9\text{S}_5$ , generally woven into network-structures. Ethylenediamine, which produced  $\text{Cu}_2\text{S}$  (monoclinic), as also  $\beta\text{-Cu}_2\text{S}$  (hexagonal), assisted formation of hexagonal micron-sized single crystal rods with a hexagonal end face in conjunction with  $\beta\text{-Cu}_2\text{S}$ .

© 2006 Elsevier Ltd. All rights reserved.

**Keywords:** A. Chalcogenides; A. Nanostructures; B. Chemical synthesis; D. Optical properties

---

## 1. Introduction

Extensive attention has been paid to the synthesis and characterization of sulphides, due to their interesting properties and potential applications.

Copper sulphides in different stoichiometries are widely used as p-type semiconductors in solar cells, as super ionic materials and as optical filters [1–2]. They are also widely applied in thin films and composite materials for their unique optical electrical properties [3–6]. Copper sulphide is often used for ammonia gas sensing at room temperature and these gas sensitive parameters have been found to be dependent upon chemical composition and the morphology of the  $\text{Cu}_x\text{S}$  materials [7,8].

Various wet chemical techniques have been employed for obtaining a variety of shapes in nanoparticles or microparticles of  $\text{Cu}_x\text{S}$  [1,6,9–14]. Previously, some researchers [12–14] including ourselves [15] reported about the synthesis of  $\text{Cu}_x\text{S}$  crystals by solvothermal/hydrothermal procedure where salts of copper (such as copper nitrate, copper chloride, copper sulphate) were used as the precursor of copper.

In the present work, as compared to the above, we used an unexplored combination for synthesis where instead of copper salt, copper metal foils were employed as the source of Cu as also as the substrate for growth and different solvents were used for gathering an idea about their roles in shape control of  $\text{Cu}_x\text{S}$  ( $x \sim 2$ ). The results point towards unique and significant shape tailorabilities as a function of the selection of a solvent; the range of shapes was from

---

\* Corresponding author. Tel.: +91 33 24734971x201; fax: +91 33 24732805.

E-mail address: [mssc2@iacs.res.in](mailto:mssc2@iacs.res.in) (S. Chaudhuri).

nanoparticles and their agglomerates (solvent: water) to thread-like and net-like forms (solvent: ethanol) to well-developed rodlike single crystals (solvent: ethylenediamine). In this paper, we also report about the differences in optical properties of the synthesized copper sulphide samples as a function of composition/structure and morphology.

## 2. Experimental

About 0.49 g of Cu foil and 0.19 g of sulphur powder were put into a Teflon-lined stainless steel autoclave. This was filled up to 75% of the total volume of the Teflon cylinder with different solvents, namely: (1) water, (2) ethanol and (3) ethylenediamine (en). The autoclave was maintained at 130 °C for 12 h and subsequently cooled at room temperature. The obtained black product was washed carefully with water and ethanol. The products prepared by using water, ethanol and ethylenediamine were named as sample-I, II and III, respectively.

The samples were characterized by X-ray powder diffraction (XRD), using a Seifert (3000 P) unit with monochromatic Cu K $\alpha$  radiation (Ni filter). To determine the morphology and particle size, both scanning electron microscope (SEM, Hitachi Model S-2300) and transmission electron microscope (TEM, JEOL-2010) were used. Absorption spectra of the samples dispersed in spectroscopic grade alcohol were recorded on Hitachi U-3410 spectrophotometer.

## 3. Results and discussion

### 3.1. Crystalline product identification by XRD

The X-ray diffraction pattern (XRD) of Cu foil (which is not shown here) showed it to match well with that of the JCPDS (04-0836) pattern. The pattern indicates the sample to be apparently free from any preferred orientation but with a strong development of the (1 1 1) plane, conforming to the JCPDS standard pattern.

Water and ethanol as solvents produced well-crystallized phases, the XRD patterns (Fig. 1a and b) of which looked similar, and matched very well with that of Cu<sub>9</sub>S<sub>5</sub> (JCPDS 26-0476). When ethylenediamine was used as the solvent, the product(s) identified by XRD seemed to be Cu<sub>2</sub>S phase(s). One of them, Cu<sub>2</sub>S (JCPDS 33-0490), crystallizes in the monoclinic system with the following cell dimensions (Å):  $a = 15.235$ ,  $b = 11.885$ ,  $c = 13.496$ . This phase, though not prefixed with the term “ $\alpha$ ”, has a companion polymorphic phase called  $\beta$ -Cu<sub>2</sub>S. The  $\beta$ -polymorph crystallizes in the

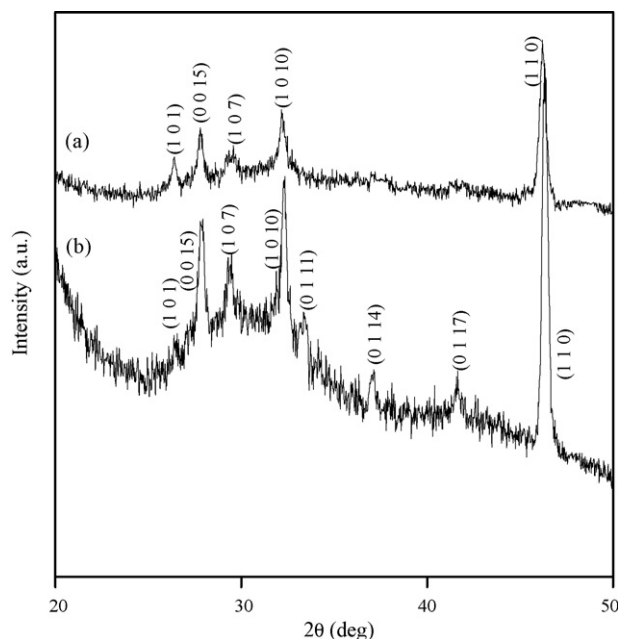


Fig. 1. XRD patterns of the reaction products obtained by using (a) water and (b) ethanol.

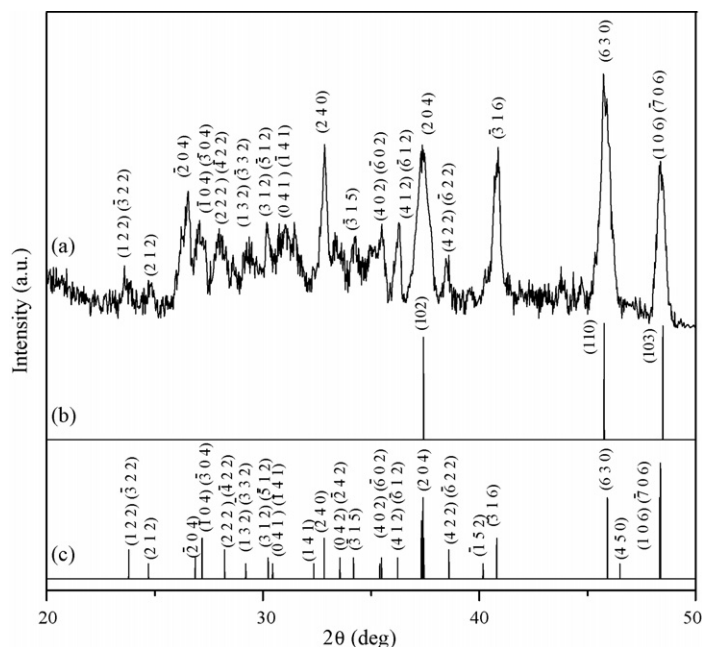


Fig. 2. (a) A typical XRD pattern of the reaction product in ethylenediamine system, (b) standard JCPDS pattern of  $\beta$ -Cu<sub>2</sub>S, and (c) standard JCPDS pattern of Cu<sub>2</sub>S.

hexagonal system with the following cell dimensions in Å (JCPDS 26-1116):  $a = 3.961$  and  $c = 6.722$ . Fig. 2 shows a typical XRD pattern obtained in this work (Fig. 2a) and the two standard patterns for  $\beta$ -Cu<sub>2</sub>S (Fig. 2b) and Cu<sub>2</sub>S (Fig. 2c). Results of slow scanning of the obtained XRD pattern in the region  $2\theta = 36.5^\circ$ – $38.5^\circ$  and  $45^\circ$ – $49^\circ$  (Cu K $\alpha$ ) are shown in Fig. 3a and b. Within the broad region of  $2\theta = 35^\circ$ – $40^\circ$ , several peaks are observed at  $37^\circ$ – $38^\circ$ : three peaks of Cu<sub>2</sub>S and one of  $\beta$ -Cu<sub>2</sub>S are known to be present in this region according to the JCPDS standard patterns. It is therefore difficult to assign any of these to the  $\beta$ -form, though the possibility of formation of both cannot be ruled out. In comparison, in case of slow scan in the range  $2\theta = 45^\circ$ – $49^\circ$ , there is a strong indication of the presence of  $\beta$ -Cu<sub>2</sub>S in the pattern, especially in the region around  $2\theta = 46^\circ$  as Cu<sub>2</sub>S has only one strong peak ( $I/I_0 = 70$ ) at  $45.921^\circ$ , and  $\beta$ -Cu<sub>2</sub>S has its strongest peak ( $I/I_0 = 100$ ) at  $45.776^\circ$ . Deconvolution of the two peaks in the region  $45^\circ$ – $46.5^\circ$   $2\theta$  (Fig. 4) clearly show the presence of two peaks at  $45.78^\circ$  and  $45.99^\circ$ . The conclusion reached is that the former peak is due to  $\beta$ -Cu<sub>2</sub>S and the latter, due to Cu<sub>2</sub>S.

### 3.2. Optical property studies

UV–vis spectrophotometry was used to characterize the absorption properties of the obtained samples. Fig. 5a presents the UV–vis spectrum of sample-I, which shows the absorption edge to be about  $\sim 690$  nm; the absorption edge of sample-II is at  $\sim 655$  nm, as shown in Fig. 5b. The absorption spectrum of sample-III (Fig. 5c) represents an absorption edge at  $\sim 1035$  nm, which is comparable with the absorption onset of bulk Cu<sub>2</sub>S (1022 nm) [6].

### 3.3. Morphological variations

It is clear from the SEM/TEM pictures shown below (Figs. 6, 8 and 9) that the three solvents yielded distinctly different morphologies of the products. These morphologies will be described here with possible routes of formation.

#### 3.3.1. Water as solvent

Water as the solvent yielded nanoparticles ( $\sim 5$ – $6$  nm) that agglomerated into large, micrometer-sized, i.e. up to  $\sim 10$   $\mu$ m particles with rounded to spherical shape, as in Fig. 6a–c. Fig. 6d indicates the high resolution

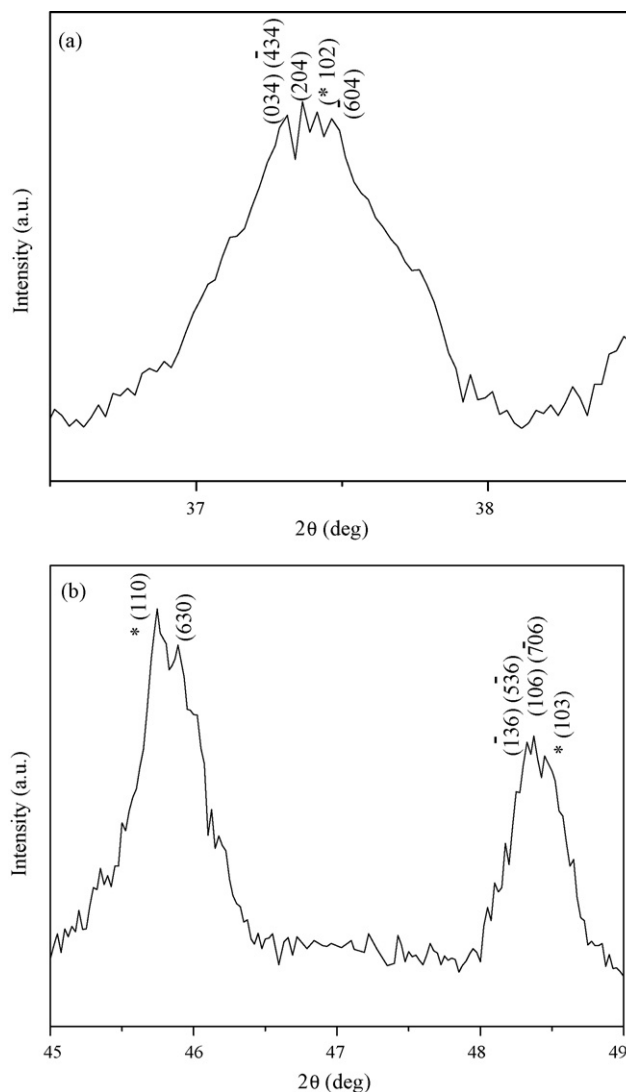


Fig. 3. Slow scan XRD patterns of the reaction product in ethylenediamine system in the region: (a) 36.5–38.5° 2θ and (b) 45–49° 2θ. \* indicates the presence of β-Cu<sub>2</sub>S.

transmission electron microscopic (HRTEM) images of the nanoparticles. The interplanar spacing was calculated and was found to be  $\sim 0.33$  nm, which corresponds to the (1 0 1) plane of Cu<sub>9</sub>S<sub>5</sub>. The most important and interesting point, however, is the nature of assemblage and specific joining of these relatively large agglomerates with formation of interfaces reminiscent of sintered products obtained through fired compacts of spherical solid particles [16]. The other parallelism is related to soap bubbles in random cellular networks [17], and their similarity with grain growth in metals [18]. Both the forms are expressions of their tendency to minimize the available surface area or energy. Fig. 7 shows a general picture of some of the aspects of such cases. In the present case, each micron-sized particle is composed of a large number of nanosized particles which do not show localized agglomeration or growth; this indicates the initial generation of a large number of nuclei and their limited growth because of necessarily restricted material supply [19]. It is observed from Fig. 6 that the dihedral angles are quite large [20], going from about 80° to 120°. In terms of sintering, this can indicate at least an intermediate stage of developing contact between two (or more) spherical or spheroidal particles through material migration, as during the initial stage [16], there should generally be a neck formation and the dihedral angle should be small (Fig. 7).

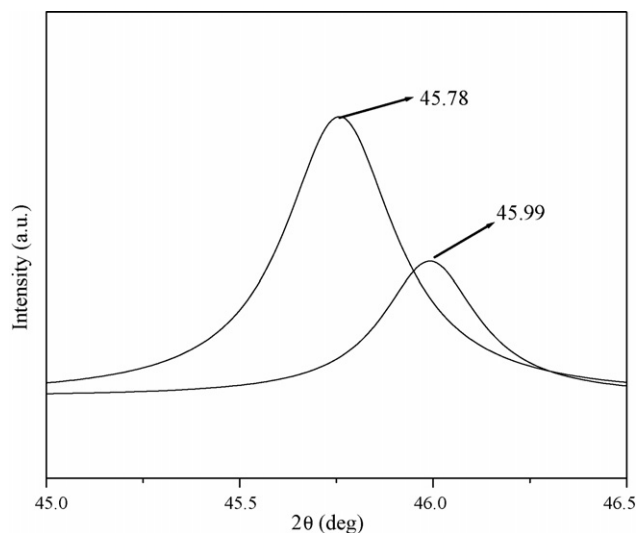


Fig. 4. Deconvoluted XRD spectrum of the reaction product in ethylenediamine system in the region  $46.0\text{--}46.6^\circ$   $2\theta$ .

The similarity of the present joining of agglomerated particles on Cu foil surface with joining via sintering practically ends here: (a) firstly, the basic starting particles in sintering are generally single crystals, polycrystals or glass or other amorphous materials, in spherical to highly irregular shapes, compacted into green bodies and (b) secondly, material exchange between two such particles in point contact (leading to neck formation [16,21]) and eventually to contact via an interface requires (generally) high thermal energy [22]. In the present case, the maximum temperature resorted to was  $130^\circ\text{C}$  and neck formation at the contact region was not noticed; further, no compaction was used, as the observed microstructure developed inside the reaction vessel.

The phenomena described here can be analyzed in the following way. The first step was formation of nuclei of copper sulphide ( $\text{Cu}_9\text{S}_5$ ) followed by growth on the copper foil, covering the available surface. A concomitant or subsequent phenomenon is continuing growth of the nuclei, but in a restricted way, because with the limited source materials, all the individual particles could not grow freely to submicron- to micron-levels [20]. As a result, further formation of nuclei and their growth could take place only on the previously deposited layer that showed preferential growth at a limited number of locations on the Cu foil. This could, among others, be guided by the polycrystalline

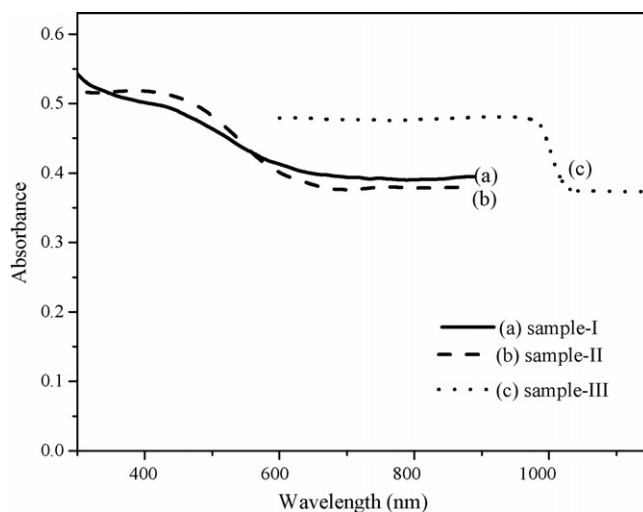


Fig. 5. UV-vis absorption spectra of copper sulphide samples prepared by solvothermal technique.

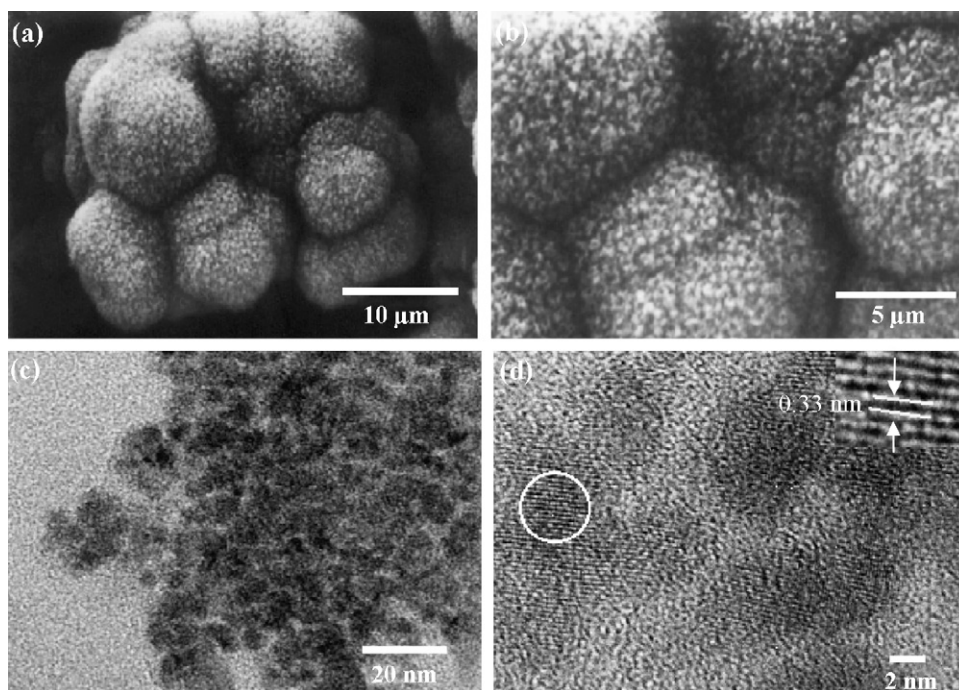


Fig. 6. Electron microscopy images of copper sulphide powders synthesized by using water as solvent: (a) low resolution SEM image, (b) higher resolution SEM image of the same sample, (c) TEM image of the same, and (d) HRTEM image of nanoparticles.

nature of the Cu foil with a number of grains and grain boundaries, and the expectedly rough surfaces of the initial spatially restricted deposits on it. These growing deposits formed hemispherical mounds, constrained to touch one another and form interfaces at a very low ( $130^{\circ}$ ) temperature.

### 3.3.2. Ethanol as solvent

The products derived from ethanol (Fig. 8) differ distinctly from those derived from water in that they are composed of porous and discontinuous networks (Fig. 8) woven of thin ( $\sim 40$  nm) fibres. Thread-like or fibre-like forms, sometimes leading to net-like forms are known in case of ethanol-mediated synthesis [23,24]. Relative solubility characteristics (e.g. polarity) of different solvents are considered to be important in determining final solid product morphologies like complex composites of one-dimensional forms [25]. It is known from available literature [26] that sulphur, a hydrophobic substance, is insoluble in water ( $\epsilon = 80.10$ ), slightly soluble in ethanol ( $\epsilon = 25.3$ ), and highly soluble in  $\text{CS}_2$  ( $\epsilon = 2.63$ ) and benzene ( $\epsilon = 2.28$ ) [27]. This is likely to be an indication that in the present case (with water and ethanol as solvents), ethanol may lead to the formation of complex one-dimensional forms, while water is not expected to do so.

### 3.3.3. Ethylenediamine as solvent

It has been already indicated above that the crystals formed through solvothermal treatment involving ethylenediamine could be both monoclinic  $\text{Cu}_2\text{S}$  and  $\beta\text{-Cu}_2\text{S}$ , which crystallized in the hexagonal system.

A literature scan shows that products of hydrothermal/solvothermal synthesis need not necessarily be only one compound. Examples are co-synthesis of  $\text{Ni}_3\text{S}_2$  and  $\text{NiS}$  [28], both rhombohedral and hexagonal polymorphs of  $\text{NiS}$  [29] and polymorphs of zirconia [30].

Fig. 9a shows predominant growth of microrods of  $5\text{--}10\text{ }\mu\text{m}$  length from the copper foil surface; the end faces of most of these microrods are hexagonal. The hexagons are not always regular, with two opposite edges sometimes differing in length from the other four. The single crystalline nature of these rods was confirmed through selected area electron diffraction analysis (Fig. 9b).

The typical morphological pattern discussed above should be related to the commonly observed templating ability of the chelating agent ethylenediamine to assist one-dimensional growth of notably oxides and sulphides [31–34]. Ethylenediamine is known to assist dissolution of sulphur [11], which has also been clearly observed in the present

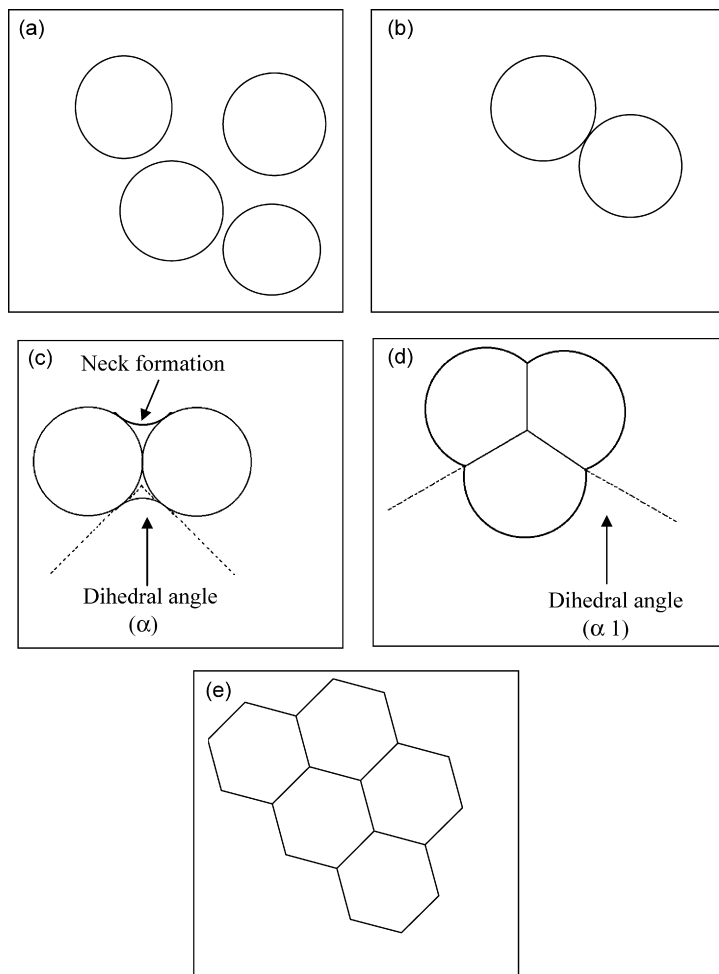


Fig. 7. Some general trends in interactions of particles: (a) particles in free movement; (b) particles in point contact, without material exchange; (c) particles initially in point contact, but forming a neck as a result of material exchange, through, e.g. evaporation–condensation, as in ceramics. Note a small dihedral angle; (d) particles forming interfaces at an advanced stage of interaction. Note a large dihedral angle; (e) a final, ideal form of connectivity, as in ceramics or foam due to aggregation of soap bubbles in a cellular network.

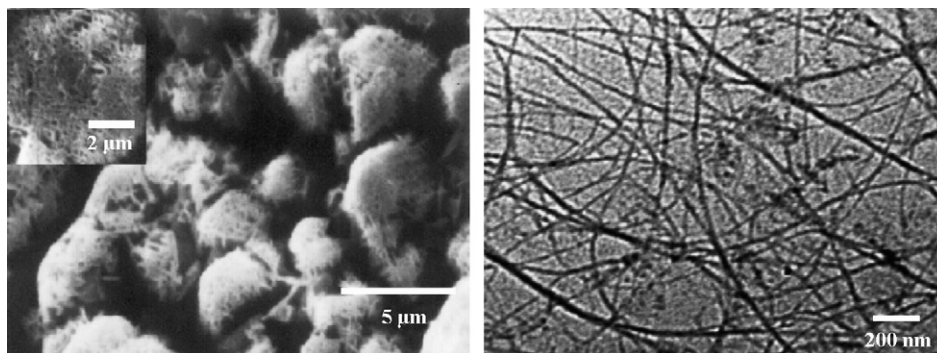


Fig. 8. Electron microscopic images of copper sulphide powders synthesized by using ethanol as solvent: (a) low resolution SEM image. Inset of the figure shows the higher resolution SEM image of it; (b) TEM image of the same sample.



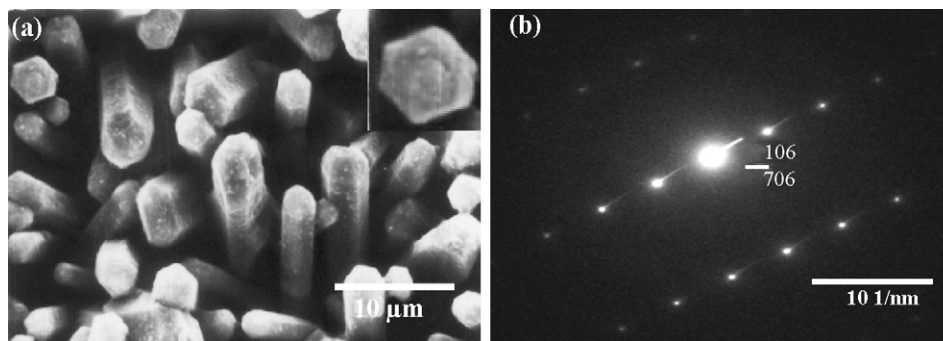
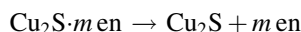
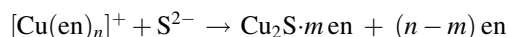
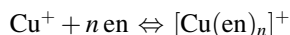


Fig. 9. (a) SEM images of copper sulphide powders synthesized by using ethylenediamine as solvent. Inset of the figure shows the hexagonal end face of a rod. (b) HRTEM image of a single rod with the corresponding SAED pattern in the inset.

work. The Cu foil reacted with the dissolved sulphur and formed  $\text{Cu}_2\text{S}$  under ionization equilibrium. The formation of  $\text{Cu}^+$  (as against  $\text{Cu}^{2+}$ ) was revealed by the formation of  $\text{Cu}_2\text{S}$ , identified as pure sulphide phase by XRD analysis:



The equilibrium was disturbed in en solution and  $\text{Cu}^+$  ion co-ordinated with en molecule to form stable  $[\text{Cu}(\text{en})_n]^+$  complex ( $k = 10^{10.8}$ ). The complex ions with bidentate ligands can be linked by the hydrogen bonds and self-assemble to form chains, which facilitates the oriented growth of  $\text{Cu}_2\text{S}$ :



At elevated temperature and pressure the stability of the above copper complex was decreased and finally at our reaction temperature (130 °C)  $\text{Cu}_2\text{S}$  was obtained.

#### 4. Conclusions

Compositions and morphological characteristics of some copper sulphides synthesized through solvothermal reactions of sulphur with a copper foil were found to be controlled basically by the solvent, when other parameters were constant. The results were:

- (1) Water as solvent led to the crystallization of  $\text{Cu}_9\text{S}_5$  agglomerated grains composed of nanoparticles; the grains formed interfaces with one another with large dihedral angles, indicating an advanced stage of connectivity.
- (2) Ethanol as solvent also yielded crystalline  $\text{Cu}_9\text{S}_5$ , but with a network morphology composed of nanofibre or nanowire nets.
- (3) Ethylenediamine produced monoclinic  $\text{Cu}_2\text{S}$ , as also hexagonal  $\beta\text{-Cu}_2\text{S}$  in the form of single crystal rods with commonly hexagonal (regular and distorted) end faces. The hexagonal symmetry of  $\beta\text{-Cu}_2\text{S}$  apparently helped ethylenediamine to form the typical one-dimensional morphology with hexagonal structure.

#### References

- [1] K. Tang, D. Chen, Y. Liu, G. Shen, H. Zheng, Y. Qian, J. Cryst. Growth 263 (2004) 232.
- [2] Y. Zhang, Z. Qiao, X. Chen, J. Mater. Chem. 12 (2002) 2747.
- [3] I. Grozdanov, M. Najdoski, J. Solid State Chem. 114 (1995) 469.
- [4] C. Nascu, I. Pop, V. Ionescu, E. Indrea, I. Bratu, Mater. Lett. 32 (1997) 73.
- [5] A.M. Hermann, L. Fabick, J. Cryst. Growth 61 (1983) 658.
- [6] P. Zhang, L. Gao, J. Mater. Chem. 13 (2003) 2007.
- [7] A. Galdikas, A. Mironas, V. Strazdiene, A. Šetkus, I. Ancutiene, V. Janickis, Sens. Actuators B 67 (2000) 76.



- [8] A. Šetkus, A. Galdikas, A. Mironas, I. Šimkiene, I. Ancutiene, V. Janickis, S. Kačiulis, G. Mattogno, G.M. Ingo, *Thin Solid Films* 391 (2001) 275.
- [9] X.H. Liao, N.Y. Chen, S. Xu, S.B. Yang, J.J. Zhu, *J. Cryst. Growth* 252 (2003) 593.
- [10] X. Wang, C. Xu, Z. Zhang, *Mater. Lett.* 167 (2002) 249.
- [11] M. Chen, Y. Xie, H. Chen, Z. Qiao, Y. Qian, *J. Colloid Interface Sci.* 237 (2001) 47.
- [12] A.-M. Qin, Y.-P. Fang, H.-D. Ou, H.-Q. Ou, H.-Q. Liu, C.-Y. Su, *Cryst. Growth Des.* 5 (2005) 855.
- [13] H. Zhu, X. Ji, D. Yang, Y. Ji, H. Zhang, *Microporous Nanoporous Mater.* 80 (2005) 153.
- [14] Y.C. Zhang, J. Qiao, X.Y. Hu, *J. Cryst. Growth* 268 (2004) 64.
- [15] S. Gorai, D. Ganguli, S. Chaudhuri, *Cryst. Growth Des.* 5 (2005) 875.
- [16] T.A. Ring, *Fundamentals of Ceramic Powder Processing and Synthesis*, Academic Press, San Diego, 1996, pp. 783–800.
- [17] F. Bolton, D. Wearie, *Philos. Mag. B* 63 (1991) 795.
- [18] D. Weaire, J.P. Kermode, *Philos. Mag. B* 48 (1983) 245.
- [19] V.K. LaMer, R.H. Dinegar, *J. Am. Chem. Soc.* 72 (1950) 4847.
- [20] A.R. West, *Solid State Chemistry and Its Applications*, John Wiley, Chichester, 1984, pp. 655–657.
- [21] Y. Wang, L. Cai, Y. Xia, *Adv. Mater.* 17 (2005) 473.
- [22] W.D. Kingery, H.K. Bowen, D.R. Uhlmann, *Introduction to Ceramics*, John Wiley and Sons, New York, 1976, pp. 448–452.
- [23] D. Chen, G. Shen, K. Tang, X. Liu, Y. Qian, G. Zhou, *J. Cryst. Growth* 253 (2003) 512.
- [24] H. Hu, Z. Liu, B. Yang, M. Mo, Q. Li, W. Yu, Y. Qian, *J. Cryst. Growth* 262 (2004) 375.
- [25] W.S. Sheldrick, M. Wachhold, *Angew. Chem. Int. Ed.* 36 (1997) 207.
- [26] *Hand book of Chemistry and Physics*, 83rd ed., CRC Press, Boca Raton, USA, 2002, pp. 4–87.
- [27] *Hand book of Chemistry and Physics*, 83rd ed., CRC Press, Boca Raton, USA, 2002, pp. 8–127.
- [28] L. Zhang, J.C. Yu, M. Mo, L. Wu, Q. Li, K.W. Kwong, *JACS* 126 (2004) 8116.
- [29] Z. Meng, Y. Peng, W. Yu, Y. Qian, *Mater. Chem. Phys.* 74 (2002) 230.
- [30] D. Ganguli, M. Chatterjee, *Ceramic Powder Preparation: A Handbook*, Kluwer Academic, Boston, USA, 1997.
- [31] H. Su, Y. Xie, Y. Xiong, P. Gao, Y. Qian, *J. Solid State Chem.* 161 (2001) 190.
- [32] A.L. Pan, R.B. Liu, S.Q. Wang, Z.Y. Wu, L. Cao, S.S. Xie, B.S. Zou, *J. Cryst. Growth* 282 (2005) 125.
- [33] C. An, K. Tanga, G. Shena, C. Wanga, Q. Yanga, B. Haia, Y. Qiana, *J. Cryst. Growth* 244 (2002) 333.
- [34] Q. Tang, X. Chen, T. Li, A. Zhao, Y. Qian, D. Yu, W. Yu, *Chem. Lett.* 33 (2004) 1085.